Angewandte Chemie
Eine Zeitschrift der Gesellschaft Deutscher Chemiker

Supporting Information

69451 Weinheim, Germany

Dioxygen Reactivity with a Ferrocene–Lewis Acid Pairing: Reduction to a Boron Peroxide in the Presence of Tris(pentafluorophenyl)borane**

*Justin T. Henthorn and Theodor Agapie**

ange_201408462_sm_miscellaneous_information.pdf

Supporting Information

Contents

General considerations:

Unless indicated otherwise, reactions performed under inert atmosphere were carried out in oven-dried glassware in a glovebox under a nitrogen atmosphere purified by circulation through RCI-DRI 13X-0408 Molecular Sieves 13X, 4x8 Mesh Beads and BASF PuriStar® Catalyst R3-11G, 5x3 mm (Research Catalysts, Inc.). Anhydrous dichloromethane was purified by sparging with nitrogen for 15 minutes and then passing under nitrogen pressure through a column of activated A2 alumina (Zapp's). CD_2Cl_2 was purchased from Cambridge Isotope Laboratories, dried over calcium hydride, then degassed by three freeze-pump-thaw cycles and vacuum-transferred prior to use. ^1H and ^{19}F NMR spectra were recorded on Varian Mercury 300 MHz spectrometers at ambient temperature, unless denoted otherwise. ^1H NMR chemical shifts are reported with respect to internal solvent: 5.32 ppm for CD_2Cl_2. ^{19}F NMR chemical shifts are reported with respect to an external standard of C_6F_6 (-164.9 ppm). Elemental analysis was conducted by Robertson Microlit Labs (Ledgewood, NJ).

Electrochemical measurements were recorded with a Pine Instrument Company AFCBP1 bipotentiostat using the AfterMath software package. Cyclic voltammograms were recorded on ca. 2 mM solutions of the relevant complex in the glovebox at 20 °C with an auxiliary Pt-coil electrode, a Ag/Ag^+ reference electrode (0.01 M $AgNO_3$, 0.1 M $[^nBu_4N^+][PF_6^-]$ in MeCN), and a 3.0 mm glassy carbon electrode disc (BASI). The electrolyte solution was 0.1 M $[^nBu_4N^+][PF_6^-]$ in CH_2Cl_2. All reported values are referenced to an internal ferrocene/ferrocenium couple.

Unless otherwise noted all chemical reagents were purchased from commercial sources and used without further purification. Ferrocene, decamethylferrocene, 2,6-di-*tert*-butyl-4-methylpyridine (DTBMP), [2.2.2]-diazabicyclooctane (DABCO) and tris(pentafluorophenyl)borane were purchased from SigmaAldrich and sublimed prior to use; $B(C_6F_5)_3$ was sublimed twice prior to use. DABCO-$2H_2O_2$ and $H(OEt_2)_2BArF^{24}$ were prepared according to the literature methods.[1,2]

NMR Scale Reactions of Cp_2Fe, Cp^*_2Fe, $B(C_6F_5)_3$, and O_2

$B(C_6F_5)_3$ and O_2: A solution of $B(C_6F_5)_3$ (0.0203 g, 0.039 mmol) in CD_2Cl_2 (0.6 mL) was degassed via three freeze-pump-thaw cycles in a J. Young NMR tube. An atmosphere of O_2 was admitted to the headspace of the tube and the reaction was continuously inverted over 24 hours at room temperature, monitoring by ^{19}F NMR spectroscopy (see **Figure S1**).

Cp^*_2Fe and O_2: A solution of Cp^*_2Fe (0.0138 g, 0.042 mmol) in CD_2Cl_2 (0.6 mL) was degassed via three freeze-pump-thaw cycles in a J. Young NMR tube. An atmosphere of O_2 was admitted to the headspace of the tube and the reaction was continuously inverted over 24 hours at room temperature, monitoring by ^1H NMR spectroscopy (see **Figure S2**).

Cp^*_2Fe and $B(C_6F_5)_3$ under N_2 – NMR: A solution of Cp^*_2Fe (0.0130 g, 0.040 mmol) and $B(C_6F_5)_3$ (0.0202 g, 0.040 mmol) in CD_2Cl_2 (0.6 mL) was added to a J. Young NMR tube and monitored over time by ^1H and ^{19}F NMR spectroscopy (see **Figure S3-4**).

Cp^*_2Fe and $B(C_6F_5)_3$ under N_2 – UV-vis: A mixed solution of Cp^*_2Fe (0.0131 g, 0.040 mmol) and $B(C_6F_5)_3$ (0.0203 g, 0.040 mmol) in DCM (1 mL) was left standing in a sealed 1 dram vial in a nitrogen filled glovebox over 26 hours at room temperature. Aliquots of the reaction were diluted by a factor of 0.06 in DCM and the formation of $Cp^*_2Fe^+$ monitored by UV-vis spectroscopy (see **Figure S6**).

Cp^*_2Fe and $B(C_6F_5)_3$ under vacuum: In the glovebox, a solution of Cp^*_2Fe (0.0133 g, 0.041 mmol) in CD_2Cl_2 (0.3 mL) was added to a J. Young NMR tube and frozen in the cold well cooled by liquid N_2. A solution of $B(C_6F_5)_3$ (0.0211 g, 0.041 mmol) in CD_2Cl_2 (0.3 mL) was layered on top of the frozen Cp^*_2Fe solution, and the tube frozen again in the cold well. The J. Young NMR tube was then sealed, removed from the glovebox and immediately submersed in an acetone/dry ice bath. The solution was degassed at -80 °C and then allowed to warm to room temperature. The reaction was monitored over time by ^1H and ^{19}F NMR spectroscopy (see **Figure S7-8**).

Cp^*_2Fe, $B(C_6F_5)_3$, and O_2: A solution of $B(C_6F_5)_3$ (0.0259 g, 0.051 mmol) and Cp^*_2Fe (0.0188 g, 0.057 mmol) in CD_2Cl_2 (0.6 mL) was degassed via three freeze-pump-thaw cycles in a J. Young NMR tube. An atmosphere of O_2 was admitted to the headspace of the tube. Upon inversion of the tube an immediate color change from yellow-orange to a dark green occurred. ^1H and ^{19}F NMR spectroscopy revealed a single new species (see **Figures S9-10**). After approximately 30 minutes a generous amount of dichroic green-blue crystals was observed in the tube.

Cp^*_2Fe, $B(C_6F_5)_3$, and O_2 in the dark: The above procedure was repeated using $B(C_6F_5)_3$ (0.0258 g, 0.051 mmol) and Cp^*_2Fe (0.0196 g, 0.057 mmol) in CD_2Cl_2 (0.6 mL) with the modification that the J. Young tube was wrapped in aluminum foil to prevent the admittance of any light into the reaction, and the lights were turned off to prevent exposure during transfer into the NMR probe. The same new species was observed by ^1H and ^{19}F NMR spectroscopy as above (see **Figures S11-12**).

Cp_2Fe, $B(C_6F_5)_3$, and O_2: A solution of $B(C_6F_5)_3$ (0.0258 g, 0.050 mmol) and Cp_2Fe (0.0109 g, 0.059 mmol) in CD_2Cl_2 (0.6 mL) was degassed via three freeze-pump-thaw cycles in a J. Young NMR tube. An atmosphere of O_2 was admitted to the headspace and the reaction was inverted continuously and monitored by ^1H and ^{19}F NMR spectroscopy over time. After 7 hours at room temperature the solution had darkened to a deep blue and all of the $B(C_6F_5)_3$ had been consumed and a single major new species was observed by ^1H and ^{19}F NMR spectroscopy (see **Figures S13-14**). After degassing the solution via three freeze-pump-thaw cycles the color had turned back to green-blue and significant decomposition was observed by ^{19}F NMR spectroscopy (see **Figures S15-16**). Repeating the experiment without degassing can result in the formation of crystals suitable for X-ray diffraction.

NMR Scale Reactions in the Presence of Additives

Cp^*_2Fe, $B(C_6F_5)_3$, and O_2 with 2,6-di-tert-butyl-4-methylpyridine (DTBMP): A solution of $B(C_6F_5)_3$ (0.0213 g, 0.0416 mmol), Cp^*_2Fe (0.0142 g, 0.0435 mmol), and DTBMP (0.0084 g, 0.0409 mmol) in CD_2Cl_2 (0.6 mL) was degassed via three freeze-pump-thaw

cycles in a J. Young NMR tube. An atmosphere of O_2 was admitted to the headspace of the tube. Upon inversion of the tube an immediate color change from yellow-orange to a dark green occurred. ^1H and ^{19}F NMR spectroscopy revealed the formation of [**1**$^{2-}$][$Cp^*_2Fe^+$]$_2$ (see **Figures S17-18**).

Cp_2Fe, $B(C_6F_5)_3$ and O_2 with DTBMP in parallel with Cp_2Fe, $B(C_6F_5)_3$ and O_2: A solution of $B(C_6F_5)_3$ (0.0202 g, 0.0395 mmol), Cp_2Fe (0.0074 g, 0.0398 mmol), and DTBMP (0.0082 g, 0.0399 mmol) in CD_2Cl_2 (0.6 mL) was degassed via three freeze-pump-thaw cycles in a J. Young NMR tube. At the same time, a solution of $B(C_6F_5)_3$ (0.0214 g, 0.0418 mmol) and Cp_2Fe (0.0082 g, 0.0441 mmol) was degassed via three freeze-pump-thaw cycles in a second J. Young NMR tube. An atmosphere of O_2 was admitted to the headspace of each tube, and the reactions followed by ^1H and ^{19}F NMR spectroscopy (see **Figures S19-20**). After approximately 2 hours at room temperature, crystals of the product [**1**$^{2-}$][Cp_2Fe^+]$_2$ began forming in both tubes, complicating qualitative comparison of the rate of the two reactions by NMR spectroscopy. Overall, the reaction appears unaffected by the presence of DTBMP.

Cp_2Fe, $B(C_6F_5)_3$ and $H(OEt_2)_2BArF^{24}$: A solution of $B(C_6F_5)_3$ (0.0119 g, 0.0232 mmol), Cp_2Fe (0.0051 g, 0.0274 mmol), and $H(OEt_2)_2BArF^{24}$ (0.0017 g, 0.00168 mmol) in CD_2Cl_2 was degassed via three freeze-pump-thaw cycles. An atmosphere of O_2 was admitted to the headspace and the reaction was inverted continuously, monitoring by ^1H and ^{19}F NMR spectroscopy over time. After approximately 3 hours the $B(C_6F_5)_3$ had been converted to a mixture of [**1**$^{2-}$][Cp_2Fe^+]$_2$ and other species (see **Figures S21-22**).

Cp_2Fe, $B(C_6F_5)_3$ and $H(OEt_2)_2BArF^{24}$: The reaction was repeated as above using $B(C_6F_5)_3$ (0.0113 g, 0.0221 mmol), Cp_2Fe (0.0046 g, 0.0256 mmol), and $H(OEt_2)_2BArF^{24}$ (0.0095 g, 0.00938 mmol) in CD_2Cl_2 (0.6 mL). After approximately 2 hours the $B(C_6F_5)_3$ had been converted to a mixture of species with negligible [**1**$^{2-}$][Cp_2Fe^+]$_2$ observed (see **Figures S23-24**). Crystals formed from this reaction were identified by a preliminary crystal structure as [{$(F_5C_6)B$}$_2OH^-$][Cp_2Fe^+] in (see **Figure S36**).

Miscellaneous Reactions

*Reaction of [**1**$^{2-}$][$Cp^*_2Fe^+$]$_2$•$2CH_2Cl_2$ with $H(OEt_2)_2BArF^{24}$:* [**1**$^{2-}$][$Cp^*_2Fe^+$]$_2$•$2CH_2Cl_2$ (0.0095 g, 0.00506 mmol) was added to a solution of $H(OEt_2)_2BArF^{24}$ (0.0055g, 0.00543 mmol) in CD_2Cl_2 (0.6 mL), and the reaction products observed by ^1H and ^{19}F NMR spectroscopy (see **Figures S25-26**).

*Reaction of [**1**$^{2-}$][Cp_2Fe^+]$_2$ with $H(OEt_2)_2BArF^{24}$:* [**1**$^{2-}$][Cp_2Fe^+]$_2$ (0.0030 g, 0.00160 mmol) was added to a solution of $H(OEt_2)_2BArF^{24}$ (0.0023g, 0.00227 mmol) in CD_2Cl_2 (0.6 mL), and the reaction products observed by ^1H and ^{19}F NMR spectroscopy (see **Figures S27-28**).

Reaction of $B(C_6F_5)_3$ with DABCO•$2H_2O_2$ and DABCO: $B(C_6F_5)_3$ (0.0221 g, 0.0432 mmol) was added to a solution of DABCO•$2H_2O_2$ (0.0020 g, 0.0111 mmol) and DABCO (0.0016 g, 0.0143 mmol) in CD_2Cl_2 (0.6 mL) and the reaction products observed by ^1H and ^{19}F NMR spectroscopy (see **Figures S29-30**).

Synthesis of bis(decamethylferrocenium) bis(tris(pentafluorophenyl)boranyl)peroxide $[1^{2-}][Cp^*_2Fe^+]_2 \bullet 2CH_2Cl_2$

$B(C_6F_5)_3$ (0.1336 g, 0.261 mmol) and Cp^*_2Fe (0.0861 g, 0.264 mmol) were combined in DCM (2 mL) and added to a Schlenk tube charged with a stir bar. The tube was then removed from the glovebox and taken to the Schlenk line where the solution was degassed via three freeze-pump-thaw cycles. Next, an atmosphere of O_2 was added to the headspace with rapid stirring. After 5 seconds the solution had turned from yellow-orange to deep forest green. After 2 minutes the stirring was stopped and the solution left standing at room temperature. After 10 minutes at room temperature dichroic crystals began forming. After 30 minutes at room temperature the solution was degassed via three freeze-pump-thaw cycles, and the Schlenk tube was taken back into the glovebox and the crystals collected on a medium porosity glass frit, washing with minimal amounts of cold DCM. The crystals were then dried under vacuum to yield 0.1297g (53.9%) of the titular compound. ^{1}H NMR (300 MHz, CD_2Cl_2 , 25 °C): δ -34.7 ppm (br). ^{19}F NMR (125 MHz, CD_2Cl_2 , 25 °C): δ -130.0 (br), -164.7 (br), -168.0 (br). λ_{max} (DCM, nm), ε ($M^{-1}cm^{-1}$): 780, 1091; 710, 653; 650, 444. Anal. Calcd for $[\mathbf{1}^{2-}][Cp^*_2Fe^+]_2 \bullet 2CH_2Cl_2$, $C_{78}H_{64}B_2Cl_4F_{30}Fe_2O_2$: C, 49.87; H, 3.43. Found: C, 50.04; H, 3.49.

Synthesis of bis(ferrocenium) bis(tris(pentafluorophenyl)boranyl)peroxide $[1^{2-}][Cp_2Fe^+]_2$

$B(C_6F_5)_3$ (0.0113g,) and Cp_2Fe (0.0043 g,) were combined in DCM (0.4 mL) and added to a J. Young NMR tube. The tube was removed from the glovebox and taken to the Schlenk line. The solution was degassed via three freeze-pump-thaw cycles and an atmosphere of O_2 was added to the headspace. The tube was then continuously inverted for several hours. Over the course of 30-60 minutes the solution changed from orange to green to dark blue. After 2 hours, some dark blue crystals began forming in the tube. After five hours, the reaction had gone to completion by ^{19}F NMR spectroscopy. After 7 hours, the solution was degassed via three freeze-pump-thaw cycles and taken back into the glovebox. The crystals were then collected on a medium porosity glass frit, washing with minimal amounts of cold DCM. The crystals were then dried under vacuum to yield 0.0043 g (27%) of the desired compound. ^{1}H NMR (300 MHz, CD_2Cl_2 , 25 °C): δ 31.9 ppm (br). ^{19}F NMR (125 MHz, CD_2Cl_2 , 25 °C): δ -139.8 (br), -165.8 (br), -172.4 (br). Anal. Calcd for $[\mathbf{1}^{2-}][Cp_2Fe^+]_2 \bullet CH_2Cl_2$, $C_{57}H_{22}B_2Cl_2F_{30}Fe_2O_2$: C, 45.25; H, 1.47. Found: C, 45.13; H, 1.56.

Synthesis of ferrocenium bis(tris(pentafluorophenyl)boranyl)hydroxide $[(F_5C_6)_3B]_2OH^-][Cp_2Fe^+]$

$B(C_6F_5)_3$ (0.0113 g, 0.0221 mmol), Cp_2Fe (0.0046 g, 0.0256 mmol), and $H(OEt_2)_2BArF^{24}$ (0.0095 g, 0.00938 mmol) were combined in DCM (0.5 mL) and added to a J. Young NMR tube. The solution was degassed via three freeze-pump-thaw cycles and an atmosphere of O_2 was added to the headspace. The tube was then continuously inverted

for several hours, monitoring by ^{19}F NMR spectroscopy. After approximately 2 hours the $B(C_6F_5)_3$ had been converted to a mixture of species with negligible $[\mathbf{1}^{2-}][Cp_2Fe^+]_2$ observed. After approximately 3 hours dark blue crystals formed in the tube, and after degassing were isolated by filtration on a fine porosity glass frit, washing with minimal amounts of cold DCM. The crystals were then dried under vacuum to yield 0.0047 g (35%) of the titular compound. A single crystal X-ray diffraction study was performed on this material (Figure S36). ^1H NMR (300 MHz, CD_2Cl_2 , 25 °C): δ 30.7 ppm (br). ^{19}F NMR (125 MHz, CD_2Cl_2 , 25 °C): δ -135.2 (br), -159.1 (br), -164.7 (br).

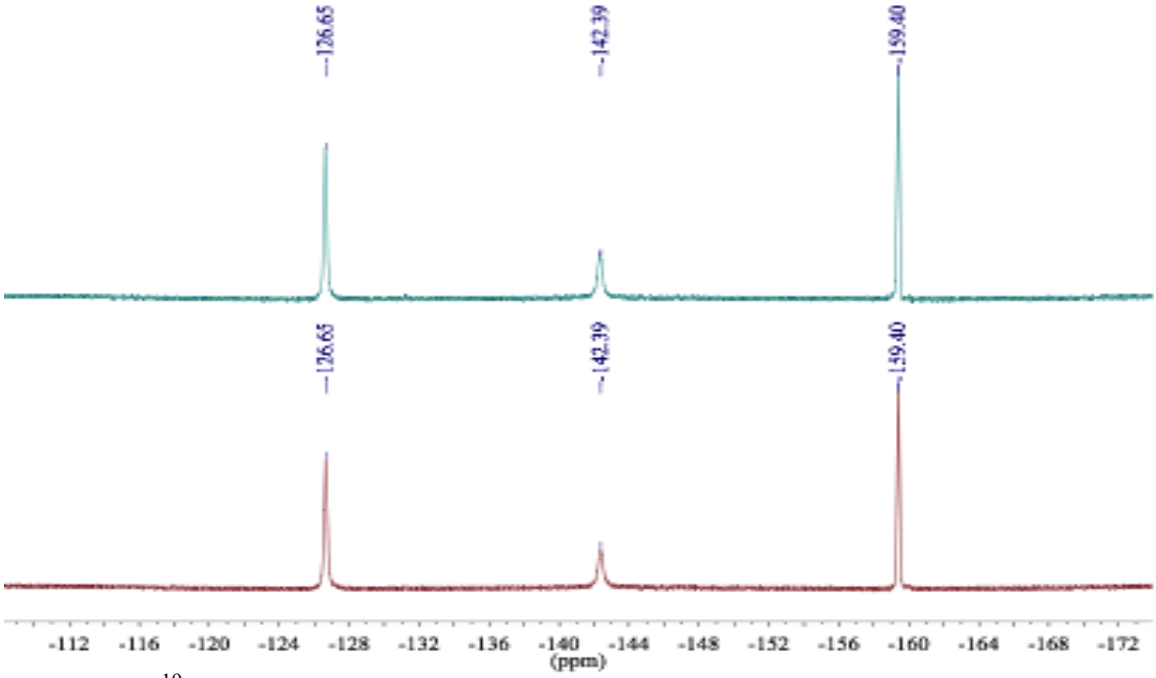

Figure S1. ^{19}F NMR spectra of $B(C_6F_5)_3$ under O_2 (1 atm) at 5 min. (bottom) and 24 hours (top) in CD_2Cl_2 at 25 °C.

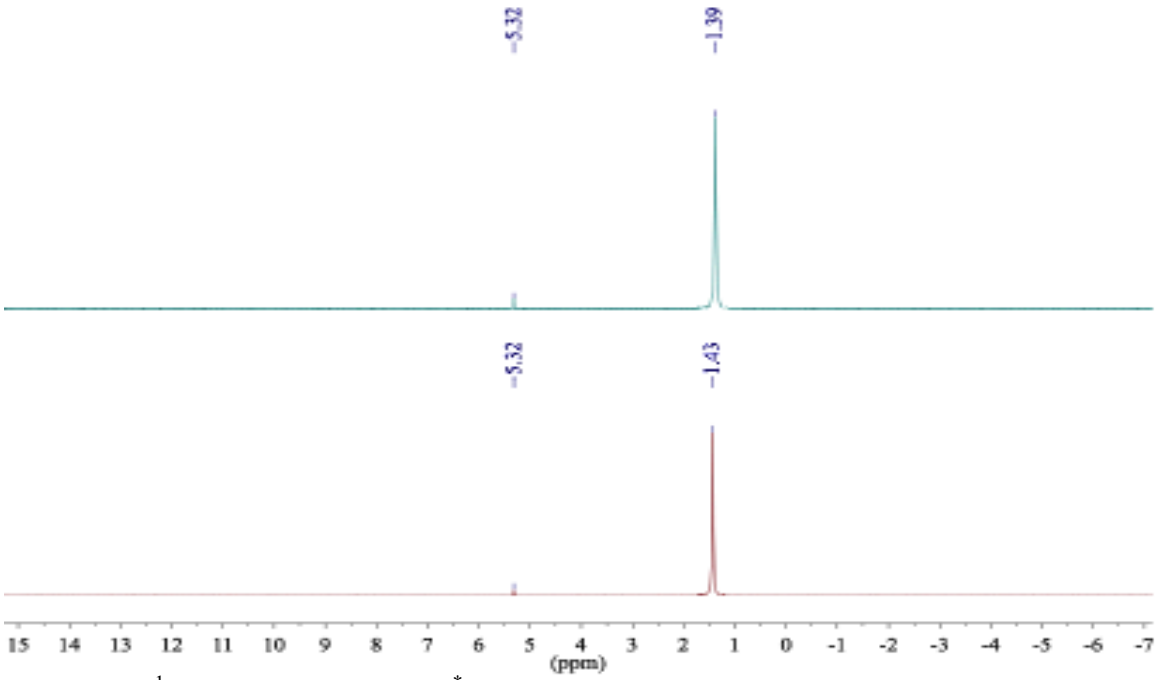

Figure S2. ^{1}H NMR spectra of Cp^*_2Fe under O_2 (1 atm) at 5 min. (bottom) and 24 hours (top) in CD_2Cl_2 at 25 °C.

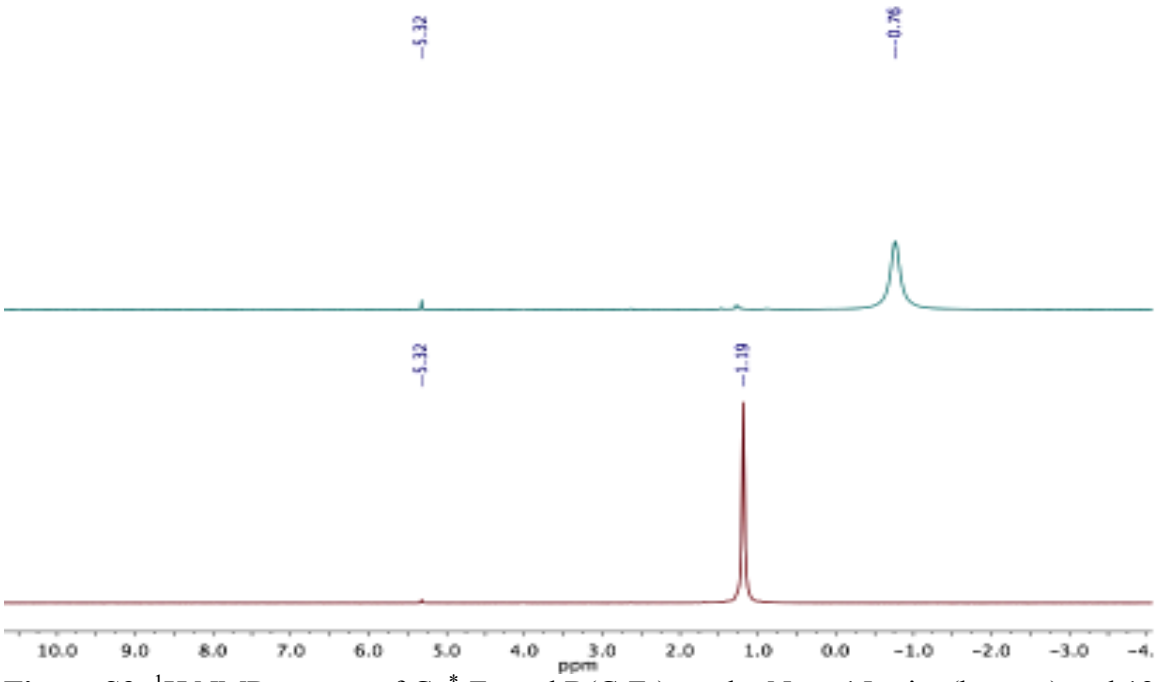

Figure S3. ^{1}H NMR spectra of $Cp^{*}_{2}Fe$ and $B(C_6F_5)_3$ under N_2 at 15 min. (bottom) and 12 hours (top) CD_2Cl_2 at 25 °C.

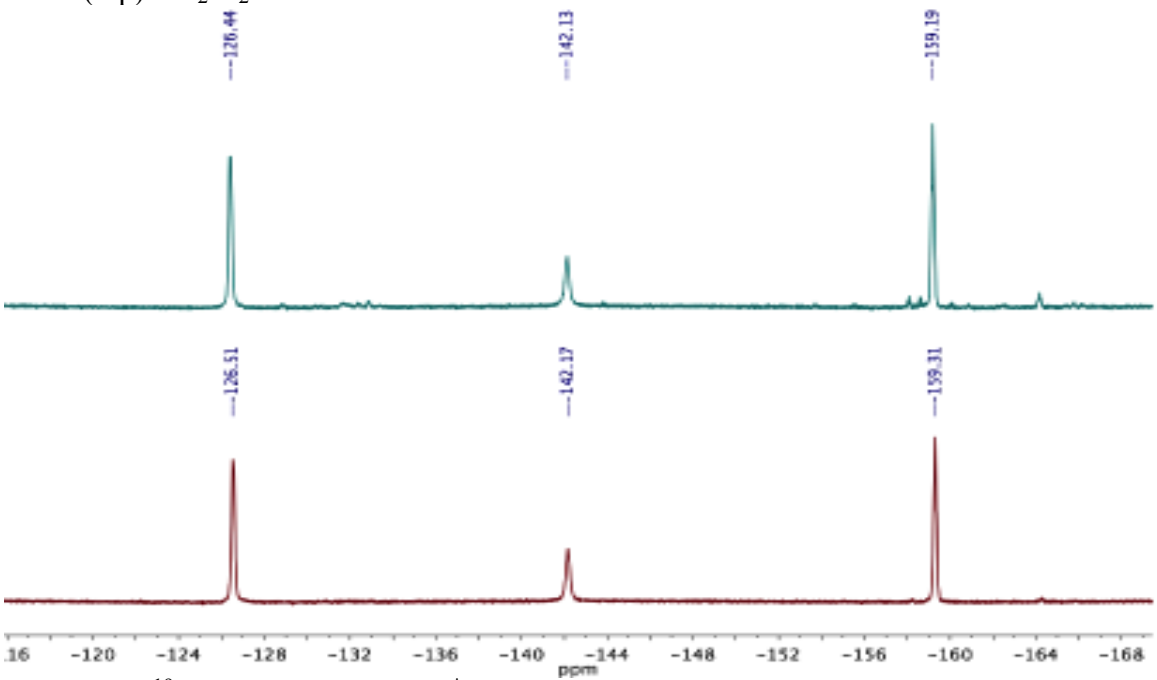

Figure S4. ^{19}F NMR spectra of $Cp^{*}_{2}Fe$ and $B(C_6F_5)_3$ under N_2 at 15 min. (bottom) and 12 hours (top) CD_2Cl_2 at 25 °C.

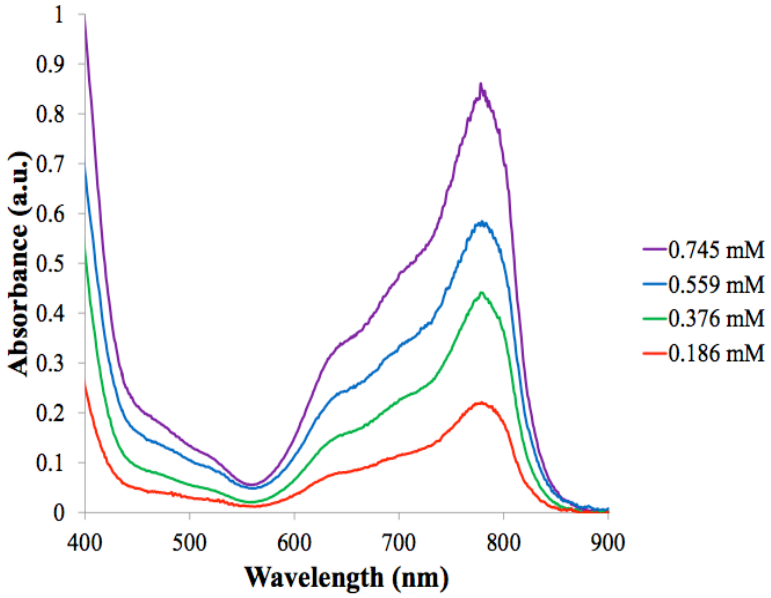

Figure S5. UV-vis spectrum of $[\mathbf{1}^{2-}][Cp^*_2Fe^+]_2$ in DCM with varying concentration.

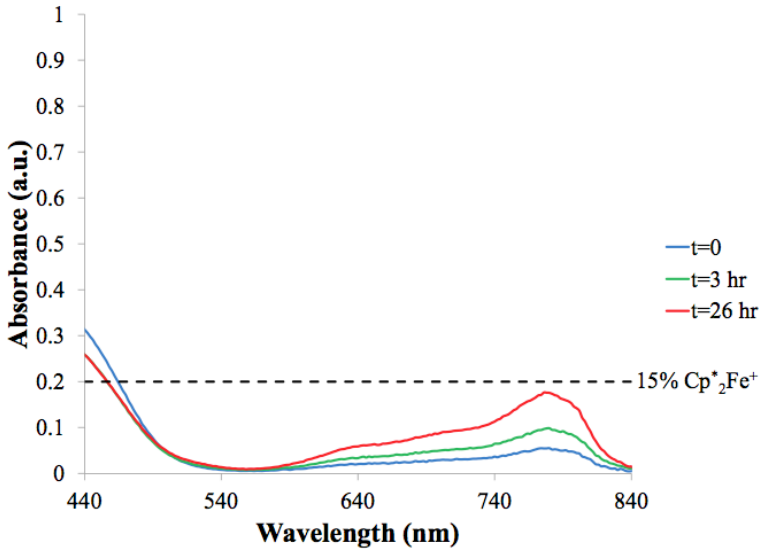

Figure S6. UV-vis monitoring of the NMR concentration reaction of Cp^*_2Fe and $B(C_6F_5)_3$ in DCM under N_2. Aliquots of the reaction were taken over time and diluted by a factor of 0.06. The absorption at 780 nm was measured to determine the amount of $Cp^*_2Fe^+$ generated. After 26 hours at room temperature, less than 15% of the total Cp^*_2Fe had been oxidized to $Cp^*_2Fe^+$.

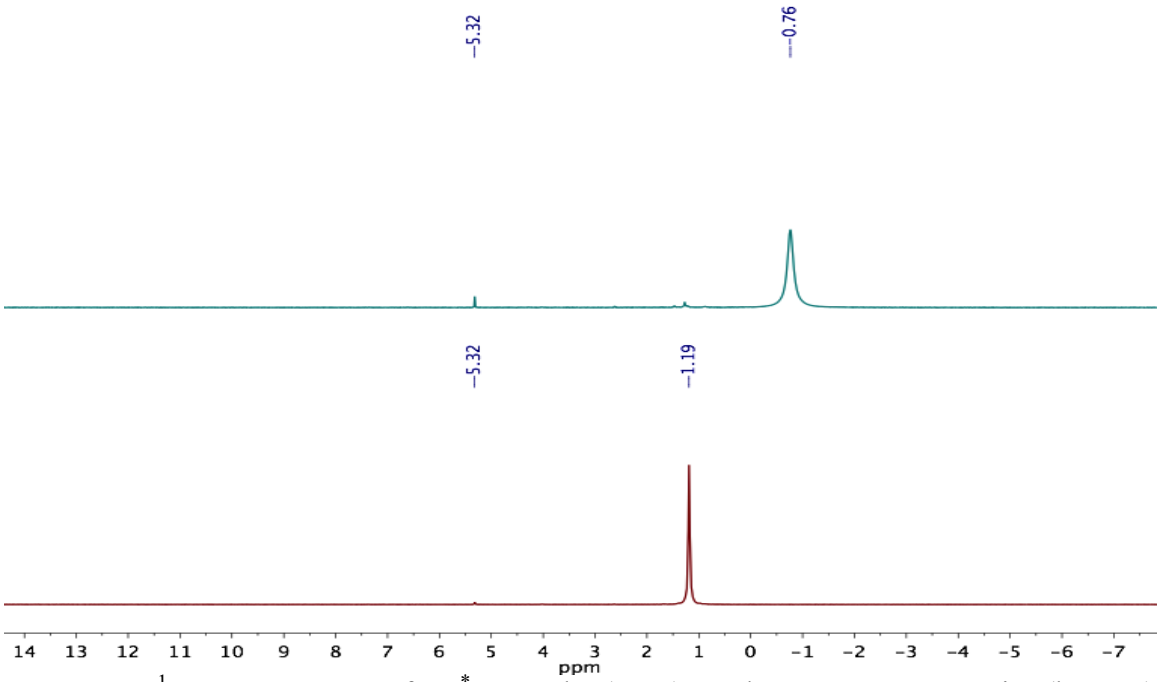

Figure S7. ^{1}H NMR spectra of $Cp^{*}_{2}Fe$ and $B(C_6F_5)_3$ under vacuum at 15 min. (bottom) and 12 hours (top) CD_2Cl_2 at 25 °C.

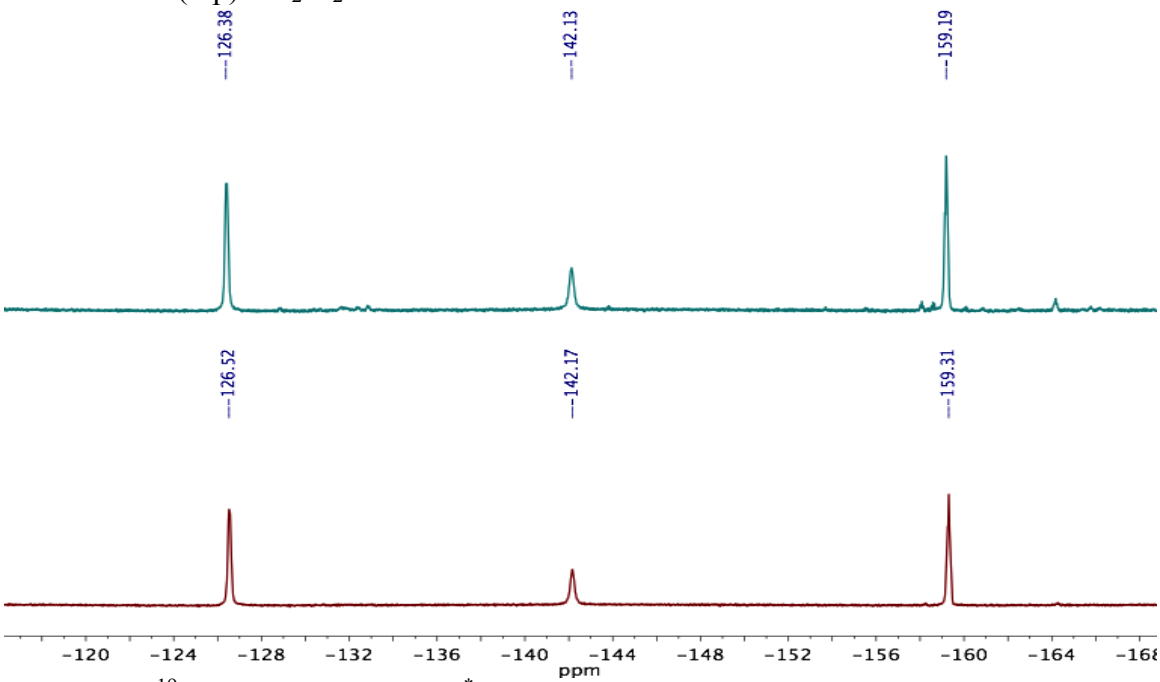

Figure S8. ^{19}F NMR spectra of $Cp^{*}_{2}Fe$ and $B(C_6F_5)_3$ under vacuum at 15 min. (bottom) and 12 hours (top) CD_2Cl_2 at 25 °C.

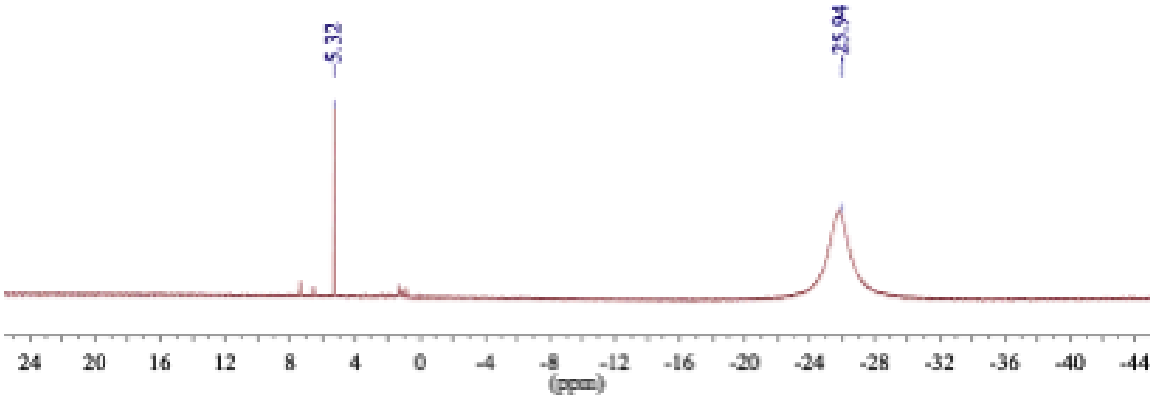

Figure S9. ^{1}H NMR spectrum of $Cp^{*}_{2}Fe$ and $B(C_6F_5)_3$ under O_2 (1 atm) in CD_2Cl_2 at 25 °C.

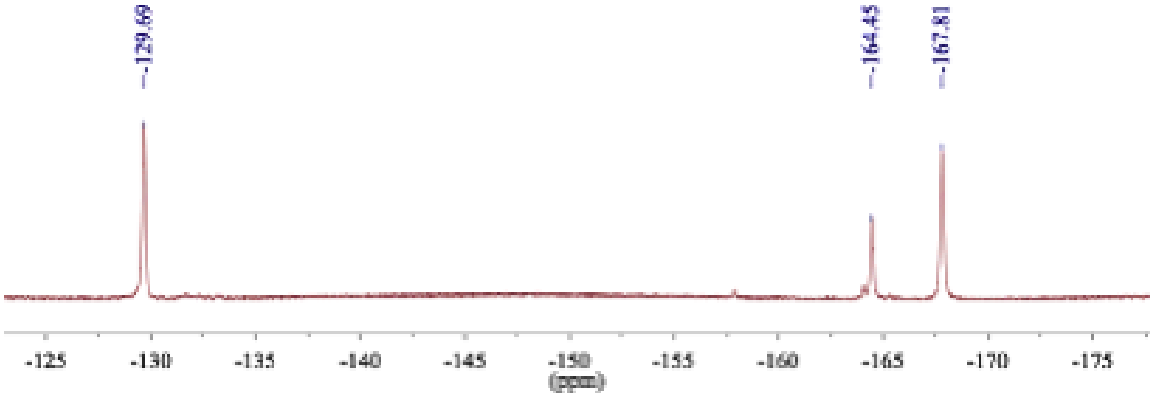

Figure S10. ^{19}F NMR spectrum of $Cp^{*}_{2}Fe$ and $B(C_6F_5)_3$ under O_2 (1 atm) in CD_2Cl_2 at 25 °C.

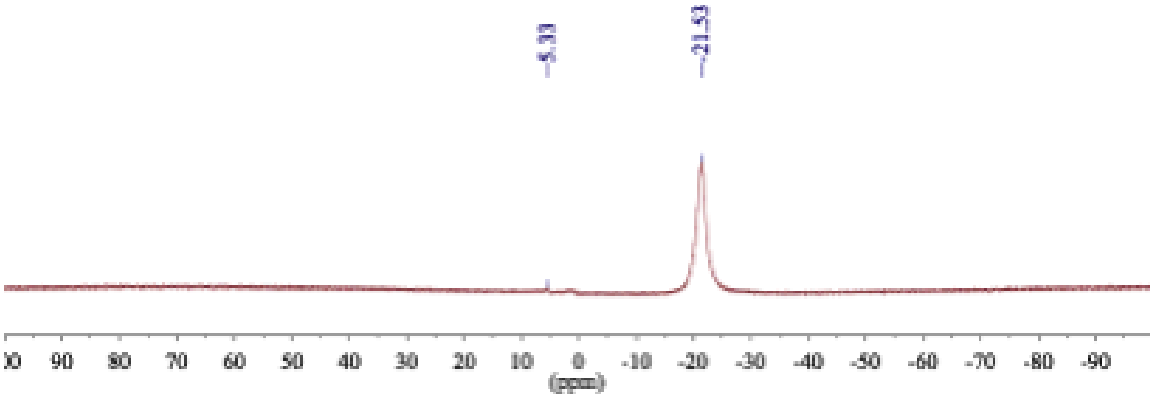

Figure S11. ^{1}H NMR spectrum of $Cp^{*}_{2}Fe$ and $B(C_6F_5)_3$ in the dark under O_2 (1 atm) in CD_2Cl_2 at 25 °C.

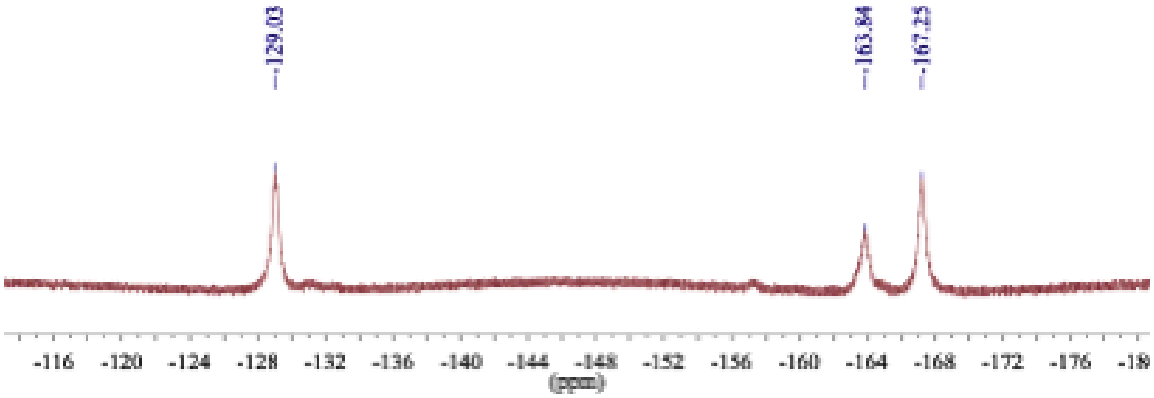

Figure S12. ^{1}H NMR spectrum of $Cp^{*}_{2}Fe$ and $B(C_6F_5)_3$ in the dark under O_2 (1 atm) in CD_2Cl_2 at 25 °C.

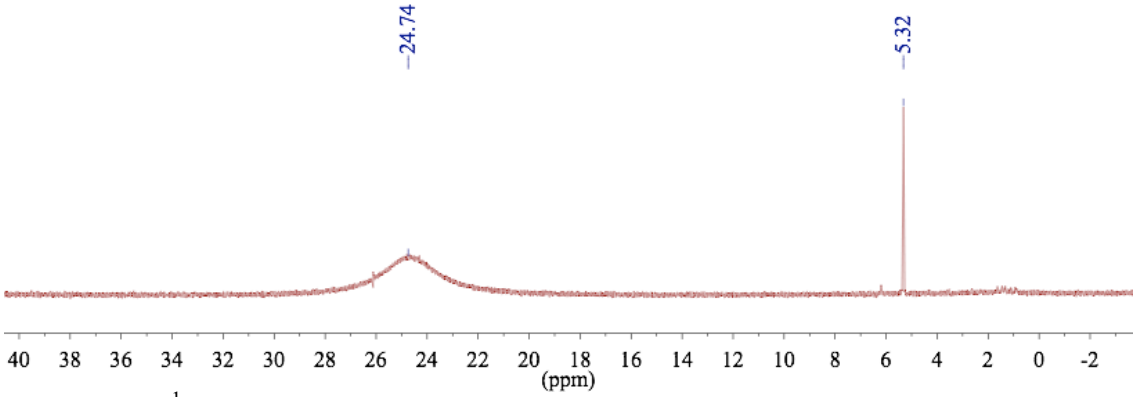

Figure S13. ^{1}H NMR spectrum of Cp_2Fe and $B(C_6F_5)_3$ under O_2 (1 atm) after 7 hours in CD_2Cl_2 at 25 °C.

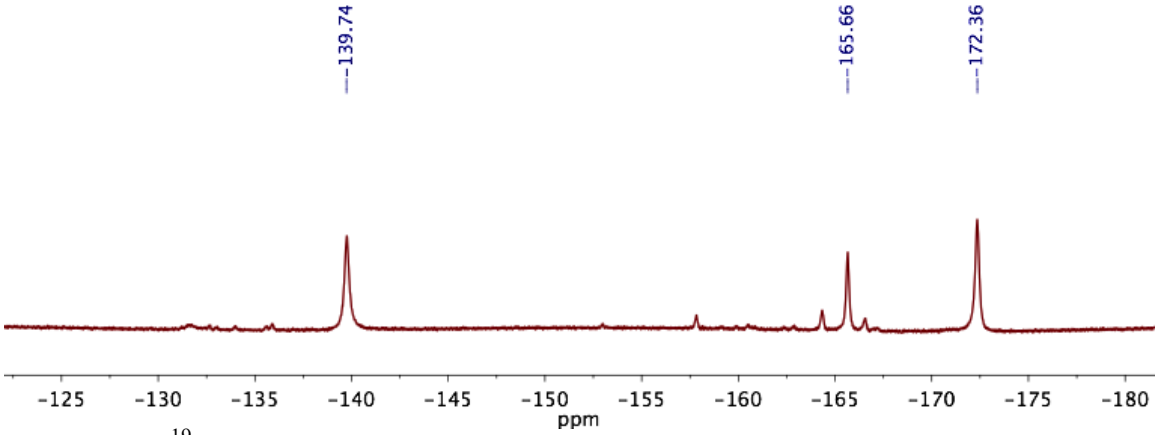

Figure S14. ^{19}F NMR spectrum of Cp_2Fe and $B(C_6F_5)_3$ under O_2 (1 atm) after 7 hours in CD_2Cl_2 at 25 °C.

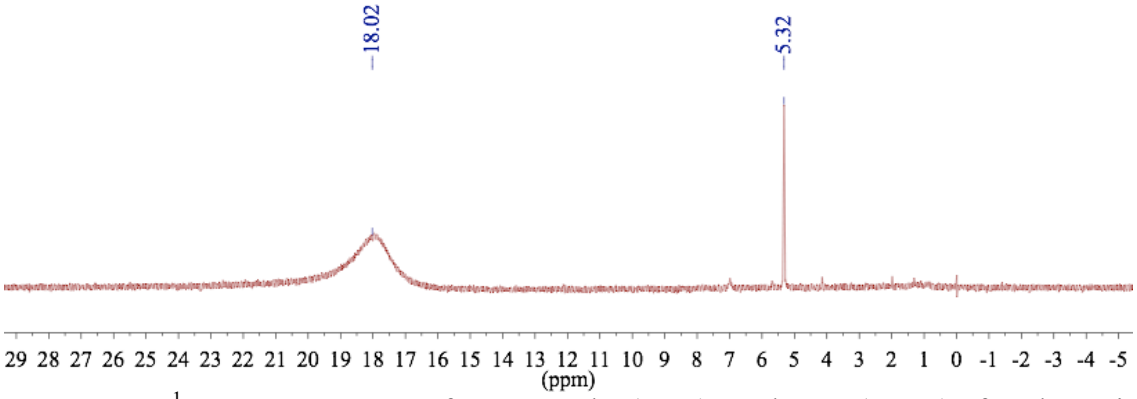

Figure S15. ^{1}H NMR spectrum of Cp_2Fe and $B(C_6F_5)_3$ under O_2 (1 atm) after degassing in CD_2Cl_2 at 25 °C.

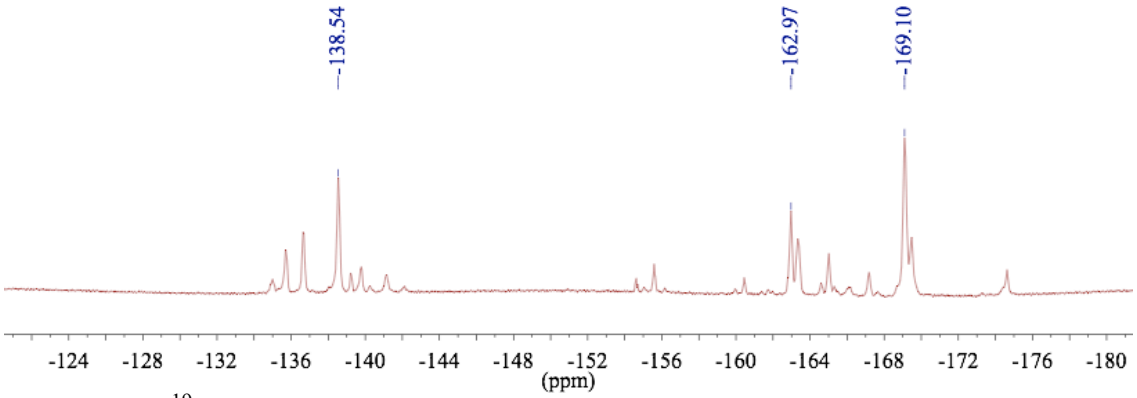

Figure S16. ^{19}F NMR spectrum of Cp_2Fe and $B(C_6F_5)_3$ under O_2 (1 atm) after degassing in CD_2Cl_2 at 25 °C.

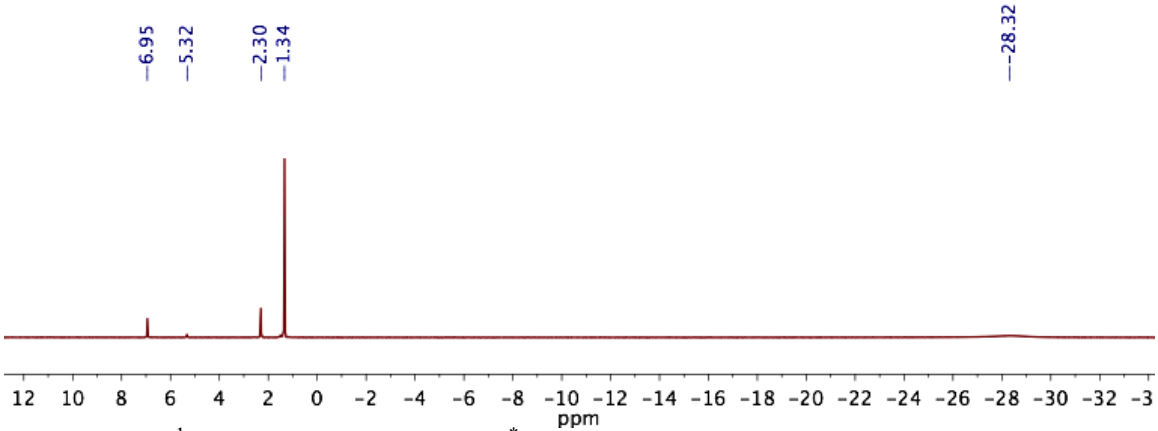

Figure S17. ^{1}H NMR spectrum of Cp^{*}_2Fe, $B(C_6F_5)_3$, and DTBMP under O_2 (1 atm) in CD_2Cl_2 at 25 °C.

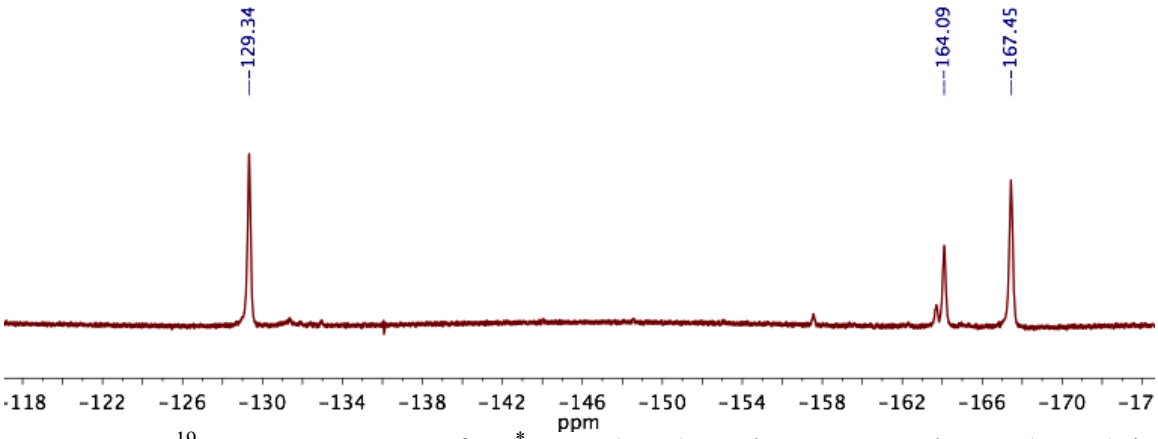

Figure S18. ^{19}F NMR spectrum of Cp^*_2Fe, $B(C_6F_5)_3$ and DTBMP under O_2 (1 atm) in CD_2Cl_2 at 25 °C.

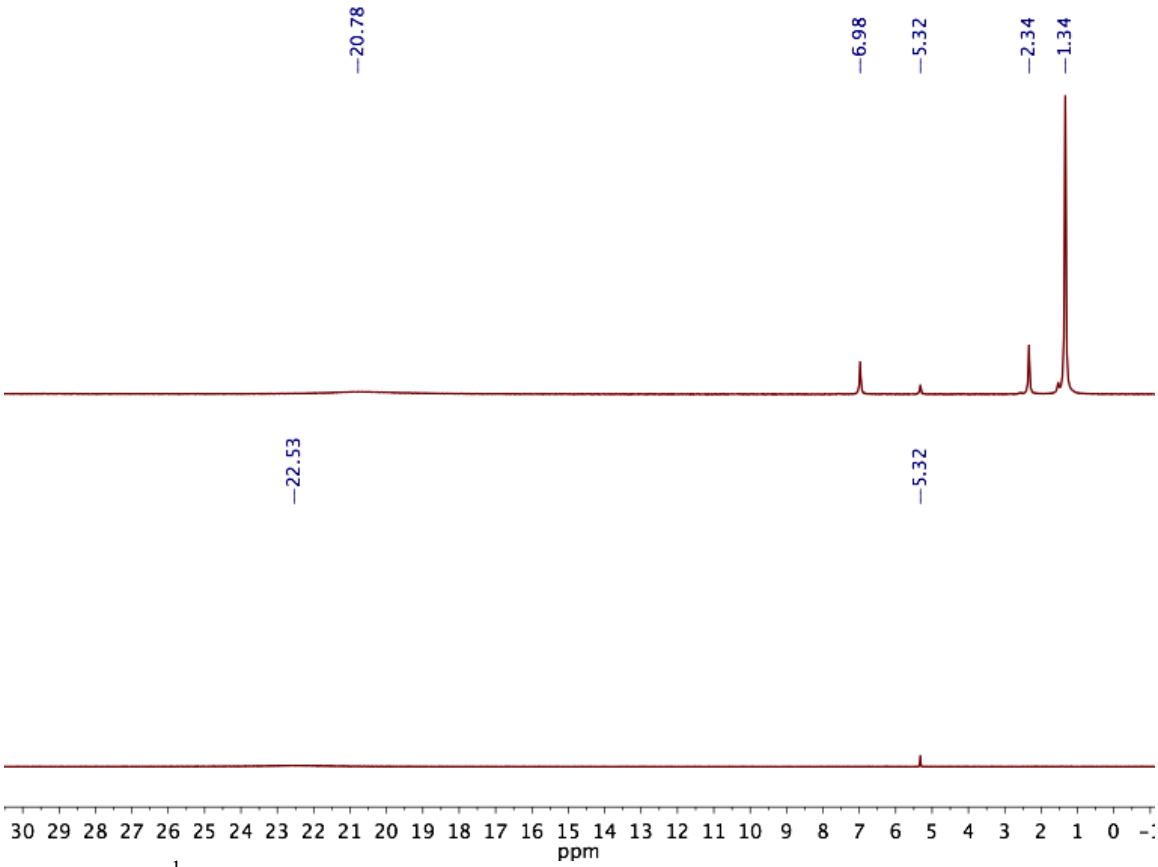

Figure S19. ^1H NMR spectrum of Cp_2Fe and $B(C_6F_5)_3$ under O_2 (1 atm) after 3 hours in CD_2Cl_2 at 25 °C (bottom) and Cp_2Fe, $B(C_6F_5)_3$ and DTBMP under O_2 (1 atm) after 3 hours in CD_2Cl_2 at 25 °C (top).

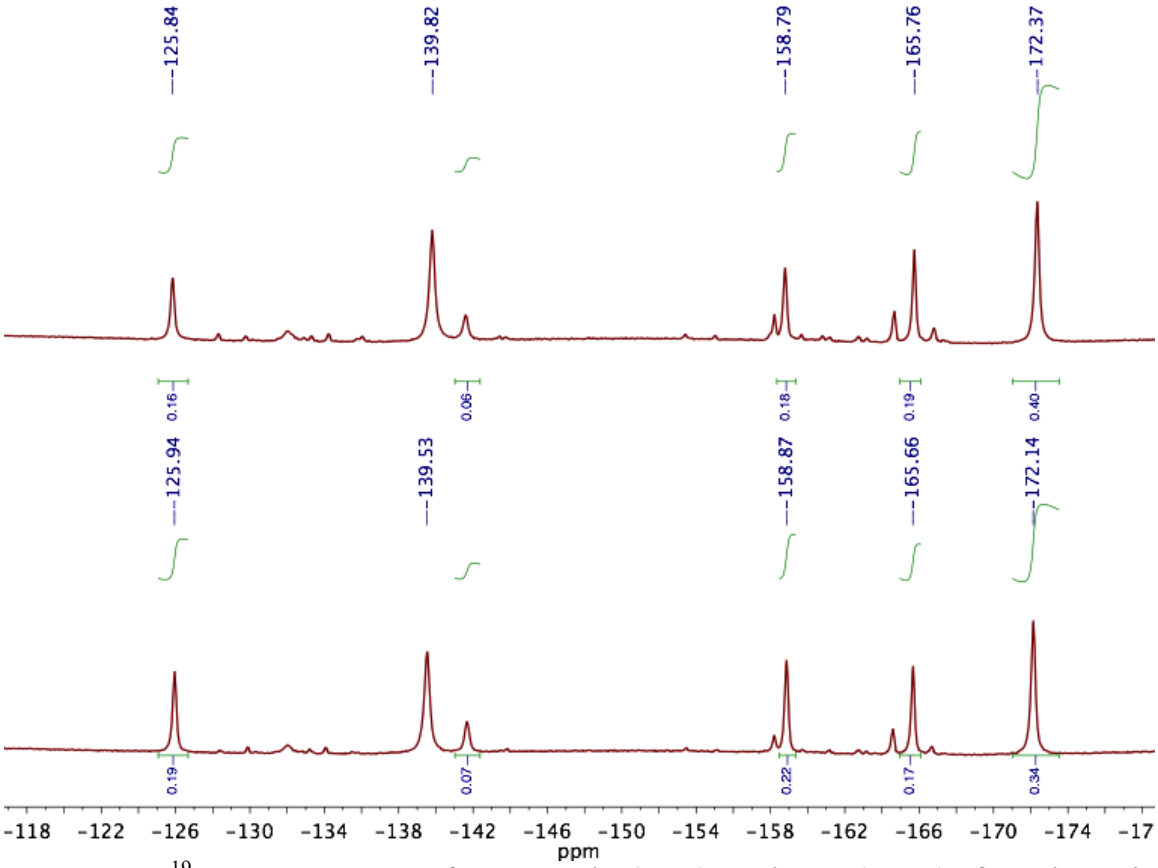

Figure S20. ^{19}F NMR spectrum of Cp_2Fe and $B(C_6F_5)_3$ under O_2 (1 atm) after 3 hours in CD_2Cl_2 at 25 °C (bottom) and Cp_2Fe, $B(C_6F_5)_3$ and DTBMP under O_2 (1 atm) after 3 hours in CD_2Cl_2 at 25 °C (top).

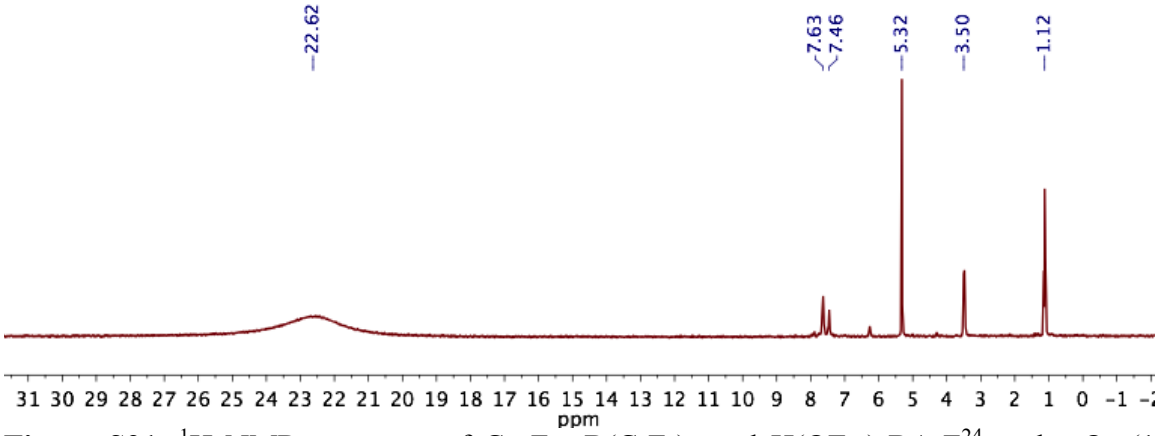

Figure S21. ^{1}H NMR spectrum of Cp_2Fe, $B(C_6F_5)_3$ and $H(OEt_2)_2BArF^{24}$ under O_2 (1 atm) after 3 hours in CD_2Cl_2 at 25 °C.

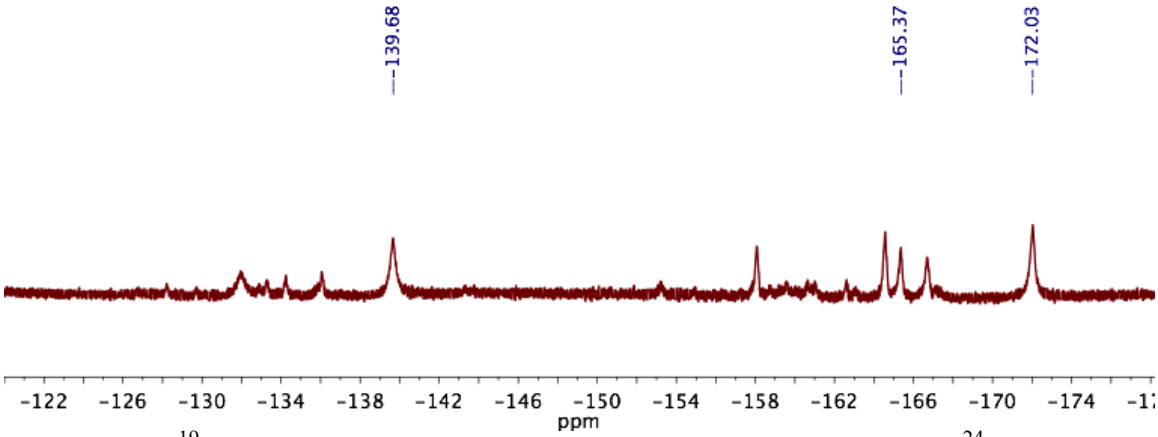

Figure S22. ^{19}F NMR spectrum of Cp_2Fe, $B(C_6F_5)_3$ and $H(OEt_2)_2BArF^{24}$ under O_2 (1 atm) after 3 hours in CD_2Cl_2 at 25 °C.

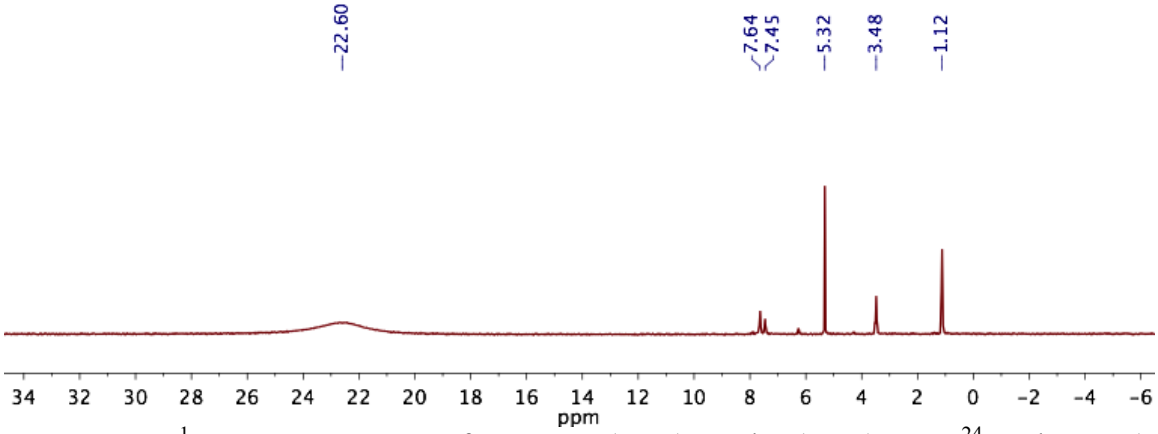

Figure S23. ^{1}H NMR spectrum of Cp_2Fe, $B(C_6F_5)_3$ and $H(OEt_2)_2BArF^{24}$ under O_2 (1 atm) after 2 hours in CD_2Cl_2 at 25 °C.

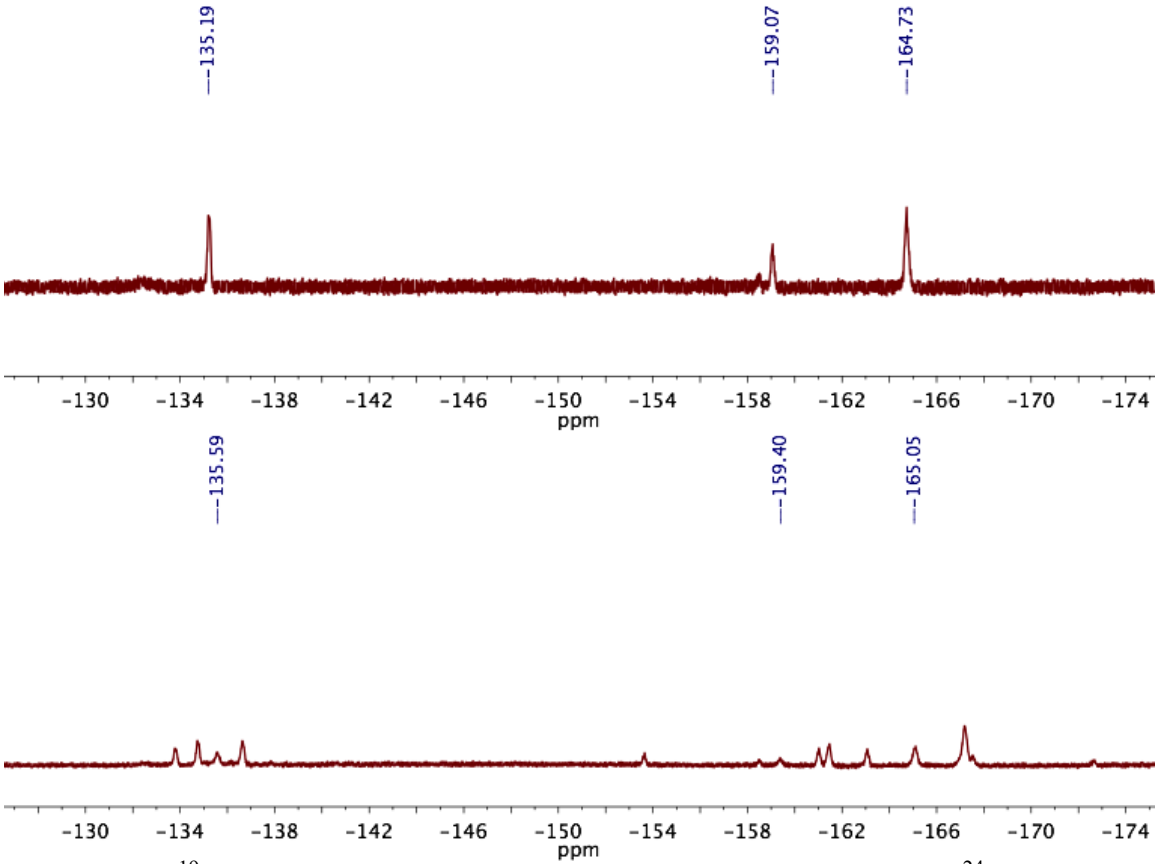

Figure S24. ^{19}F NMR spectrum of Cp_2Fe, $B(C_6F_5)_3$ and $H(OEt_2)_2BArF^{24}$ under O_2 (1 atm) after 3 hours in CD_2Cl_2 at 25 °C (bottom) and crystals of $[\{(F_5C_6)_3B\}_2OH^-][Cp_2Fe^+]$ isolated from the reaction mixture in CD_2Cl_2 at 25 °C (top).

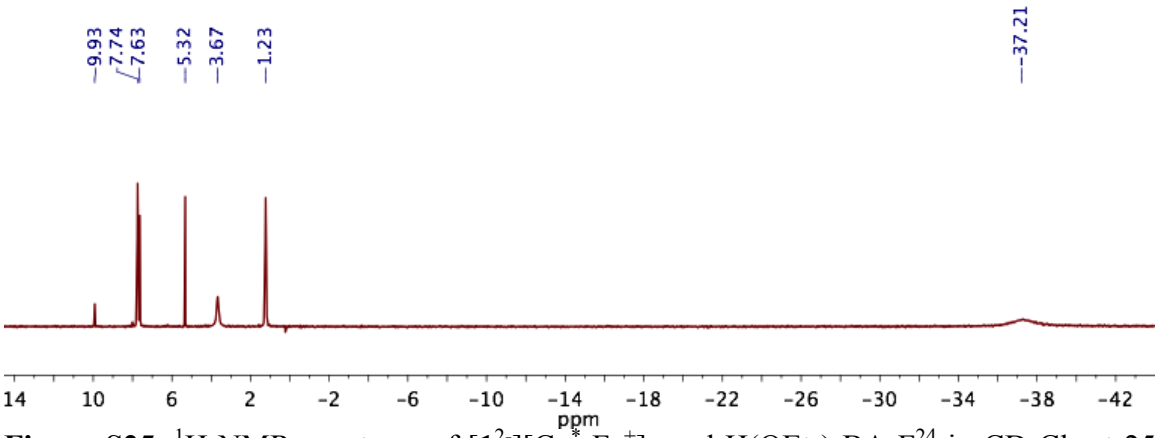

Figure S25. ^1H NMR spectrum of $[\mathbf{1}^{2-}][Cp^*_2Fe^+]_2$ and $H(OEt_2)_2BArF^{24}$ in CD_2Cl_2 at 25 °C.

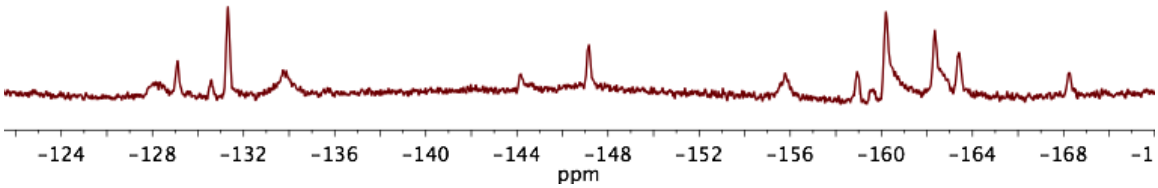

Figure S26. ^{19}F NMR spectrum of $[\mathbf{1}^{2-}][Cp^{*}_{2}Fe^{+}]_2$ and $H(OEt_2)_2BArF^{24}$ in CD_2Cl_2 at 25 °C.

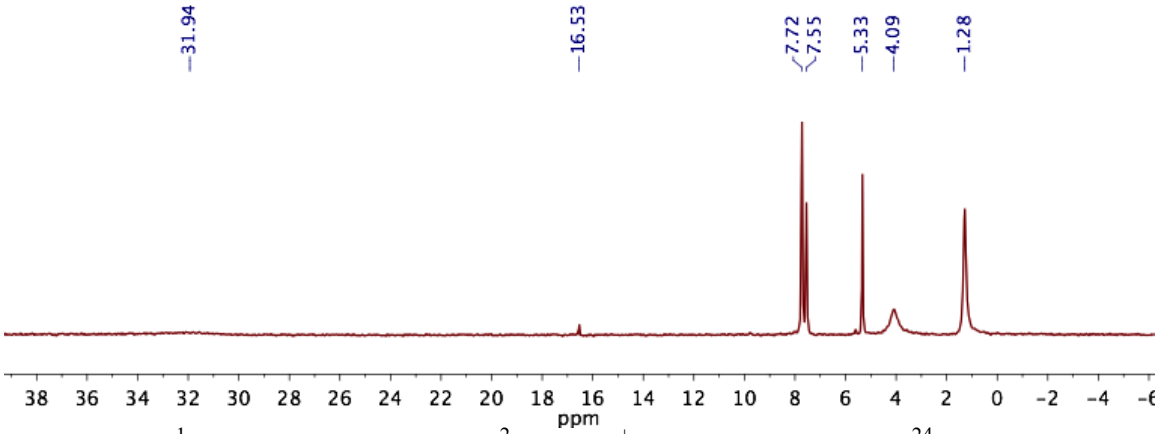

Figure S27. ^{1}H NMR spectrum of $[\mathbf{1}^{2-}][Cp_2Fe^{+}]_2$ and $H(OEt_2)_2BArF^{24}$ in CD_2Cl_2 at 25 °C.

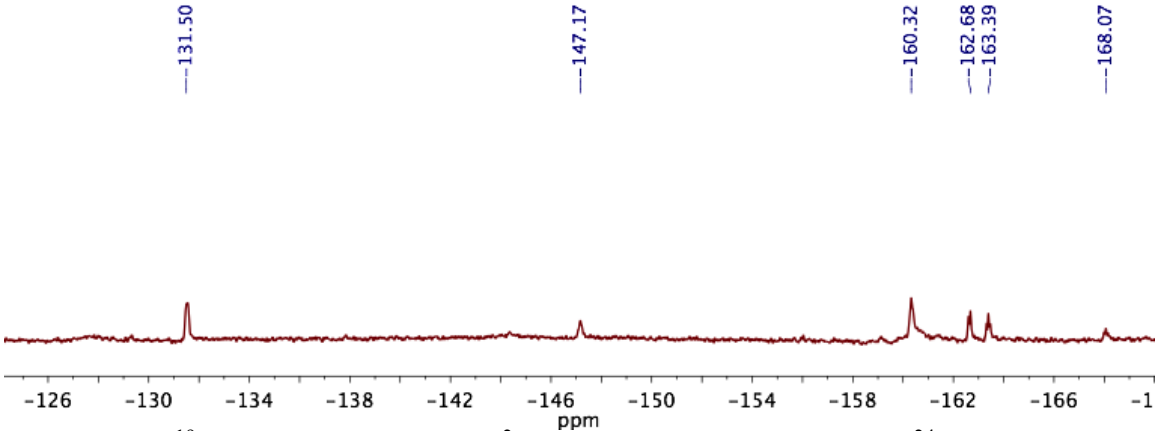

Figure S28. ^{19}F NMR spectrum of $[\mathbf{1}^{2-}][Cp_2Fe^{+}]_2$ and $H(OEt_2)_2BArF^{24}$ in CD_2Cl_2 at 25 °C.

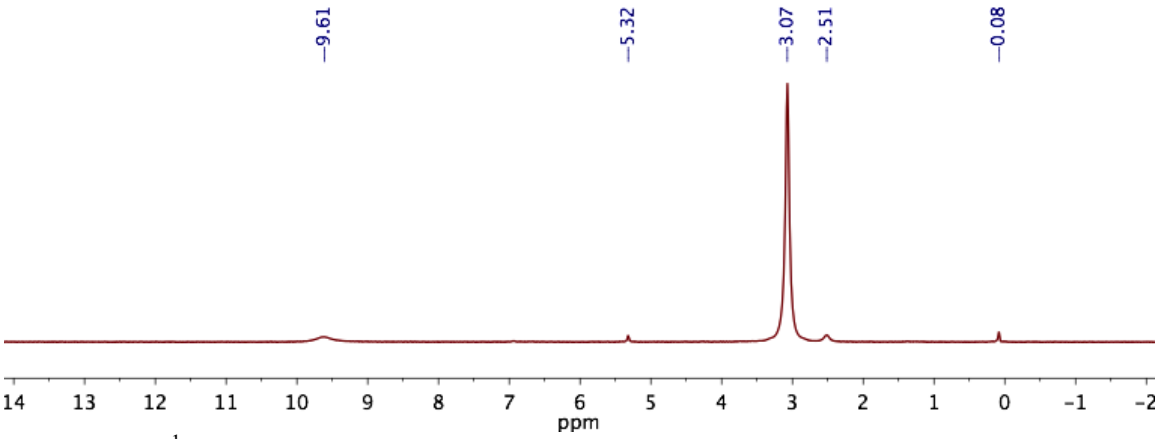

Figure S29. ^{1}H NMR spectrum of $B(C_6F_5)_3$, DABCO•$2H_2O_2$, and DABCO in CD_2Cl_2 at 25 °C.

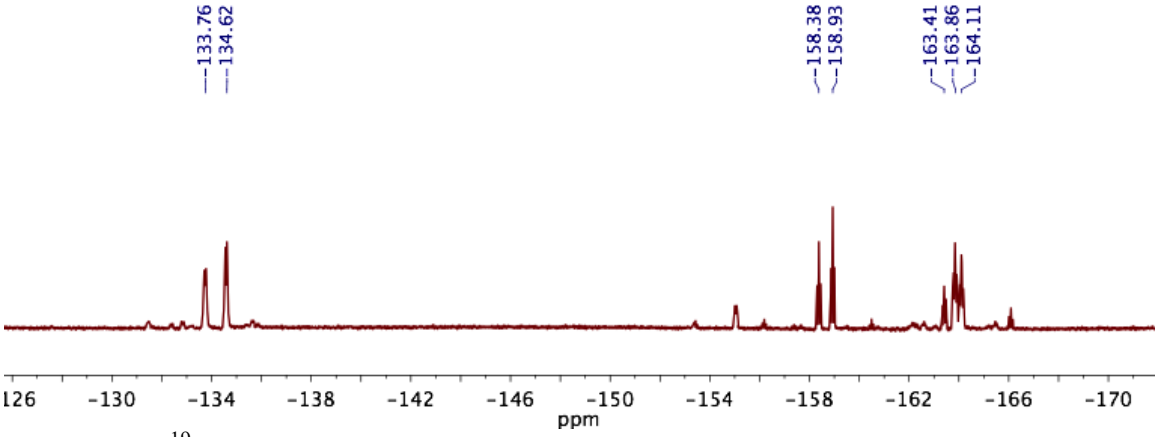

Figure S30. ^{19}F NMR spectrum of $B(C_6F_5)_3$, DABCO•$2H_2O_2$, and DABCO in CD_2Cl_2 at 25 °C.

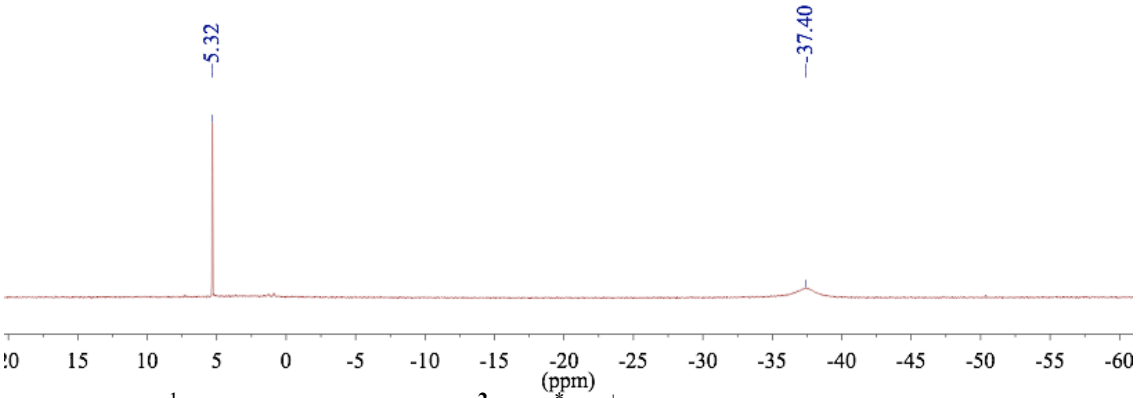

Figure S31. ^{1}H NMR spectrum of [$\mathbf{1}^{2-}$][$Cp^*_2Fe^+$]$_2$ in CD_2Cl_2 at 25 °C.

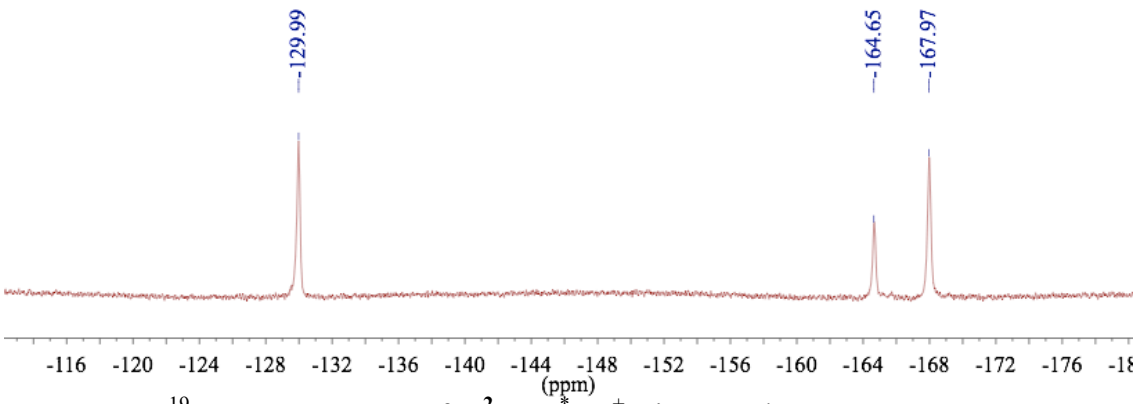

Figure S32. ^{19}F NMR spectrum of $[\mathbf{1}^{2-}][Cp^*_2Fe^+]_2$ in CD_2Cl_2 at 25 °C.

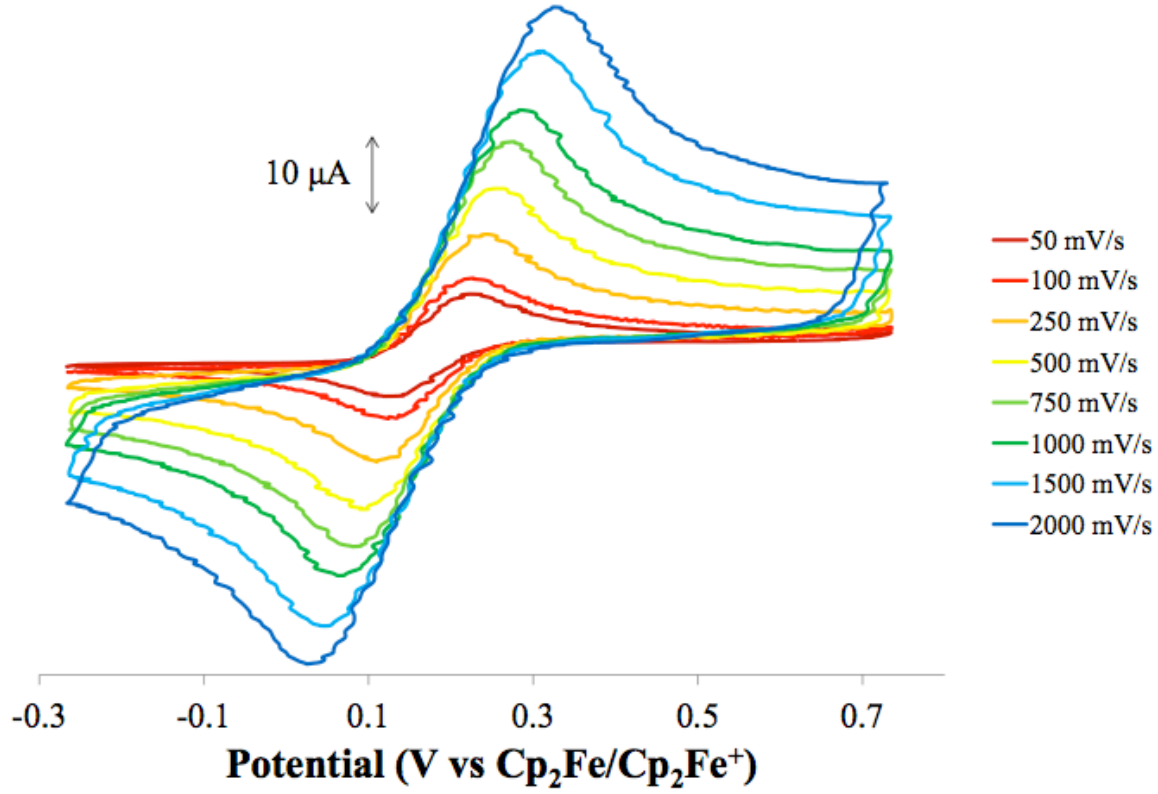

Figure S33. Variable scan rate cyclic voltammograms of $[\mathbf{1}^{2-}][Cp^*_2Fe^+]_2$ in 0.1 M $[^nBu_4N^+][PF_6^-]$ in DCM with glassy carbon electrode. Potentials referenced to Cp_2Fe/Cp_2Fe^+.

Crystallographic Information

CCDC 1000579 and 1023005 contain the supplementary crystallographic data for this paper. These data can be obtained free of charge from The Cambridge Crystallographic Data Centre via www.ccdc.cam.ac.uk/data_request/cif.

Refinement Details

In each case, crystals were mounted on a glass fiber or nylon loop using Paratone oil, then placed on the diffractometer under a nitrogen stream. Low temperature (100 K) X-ray data were obtained on a Bruker APEXII CCD based diffractometer (Mo sealed X-ray tube, K_α = 0.71073 Å) or a Bruker SMART CCD based diffractometer (Mo sealed X-ray tube, K_α = 0.71073 Å). All diffractometer manipulations, including data collection, integration, and scaling were carried out using the Bruker APEXII software.[3] Absorption corrections were applied using SADABS.[4] Space groups were determined on the basis of systematic absences and intensity statistics and the structures were solved by direct methods using XS[5] or by intrinsic phasing using XT (incorporated into SHELXTL) and refined by full-matrix least squares on F_2. All non-hydrogen atoms were refined using anisotropic displacement parameters. Hydrogen atoms were placed in the idealized positions and refined using a riding model. The structure was refined (weighed least squares refinement on F_2) to convergence. Graphical representation of structures with 50% probability thermal ellipsoids was generated using Diamond visualization software.[6]

Table 1. Crystal and refinement data for $[\mathbf{1}^{2-}][Cp^*_2Fe^+]_2 \bullet 2CH_2Cl_2$ and $[\mathbf{1}^{2-}][Cp_2Fe^+]_2$.

Compound	$[\mathbf{1}^{2-}][Cp^*_2Fe^+]_2 \bullet 2CH_2Cl_2$	$[\mathbf{1}^{2-}][Cp_2Fe^+]_2$
CCDC	1000579	1023005
empirical formula	$C_{38}H_{32}BCl_2F_{15}FeO$	$C_{28}H_{10}BF_{15}FeO$
formula wt	1878.41 g/mol	1428.04
T (K)	100	100
a, Å	11.330(2)	10.5469(9)
b, Å	14.003(3)	10.646(1)
c, Å	14.176(3)	12.043(1)
α, deg	114.17(3)	77.024(3)
β, deg	105.17(3)	88.081(4)
γ, deg	96.41(3)	71.474(3)
V, Å^3	1918.3(7)	1248.3(2)
Z	1	1
cryst syst	Triclinic	Triclinic
space group	P-1	P-1
d_{calc}, g/cm^3	1.626	1.900
θ range, deg	2.20 to 43.57	2.38 to 30.58
μ , mm^{-1}	0.639	0.742
abs cor	Multi-scan	Multi-scan
GOF[a]	0.961	0.9420
R_1[b], wR_2[c] (I > 2sig(I))	0.0599, 0.1920	0.0869, 0.2449
Diffractometer	SMART	APEXII

[a] $GOF = S = \{ \mathbf{\Sigma} [w(F_{o2}-F_c^2)^2] / (n-p) \}^{1/2}$

[b] $R1 = \mathbf{\Sigma}||F_o|-|F_c|| / \mathbf{\Sigma}|F_o|$ [c] $wR2 = \{ \mathbf{\Sigma} [w(F_o^2-F_c^2)^2] / \mathbf{\Sigma} [w(F_o^2)^2] \}^{1/2}$

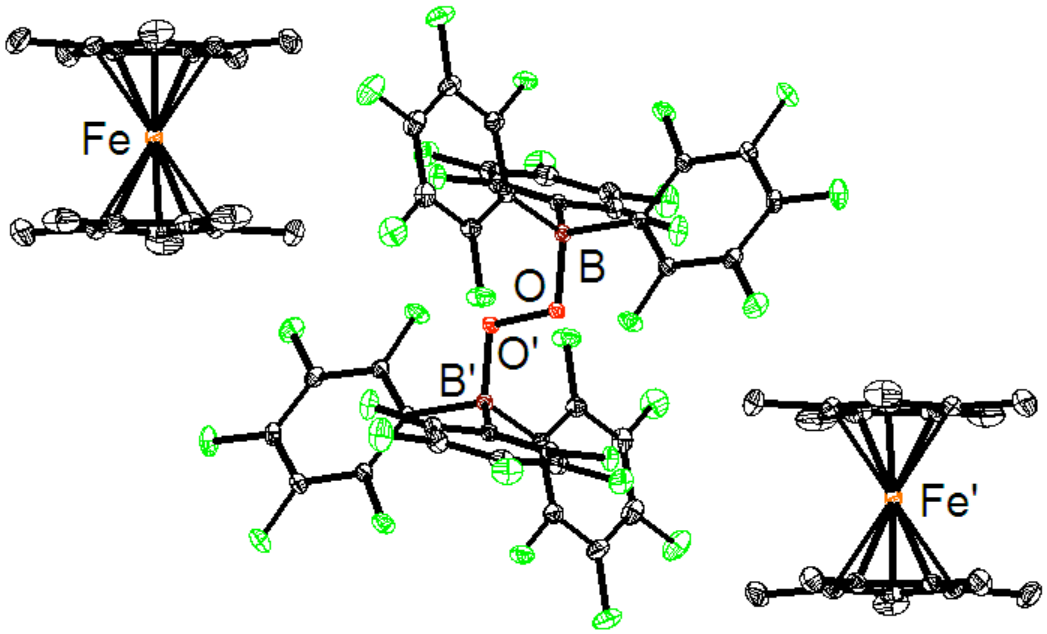

Figure S34. Structural drawing of [$\mathbf{1}^{2-}$][$Cp^{*}_{2}Fe^{+}$]$_2$•2CH_2Cl_2 with 50% probability ellipsoids. Hydrogen atoms and solvent molecules not shown for clarity. Carbon and fluorine atoms shown in black and green, respectively.

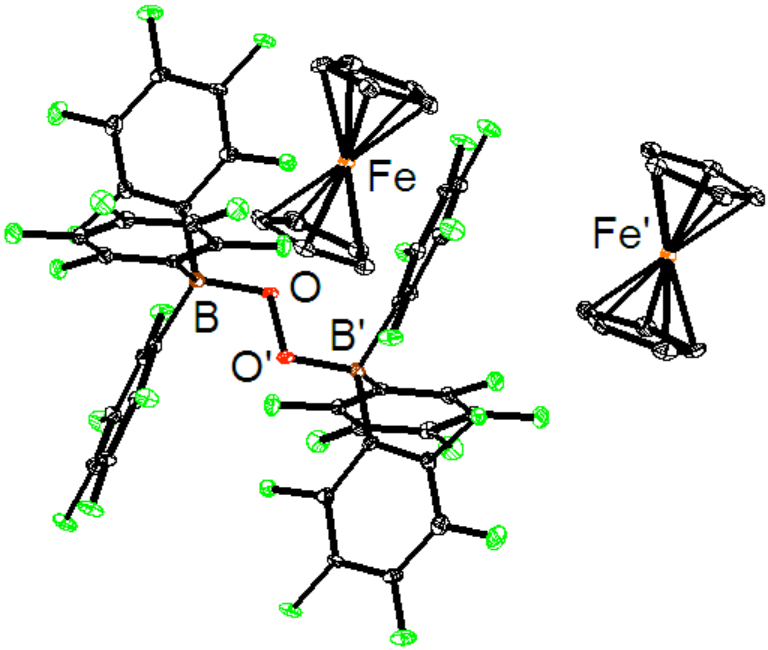

Figure 35. Structural drawing of [$\mathbf{1}^{2-}$][Cp_2Fe^{+}] with 50% probability ellipsoids. Hydrogen atoms not shown for clarity. Carbon and fluorine atoms shown in black and green,

respectively.

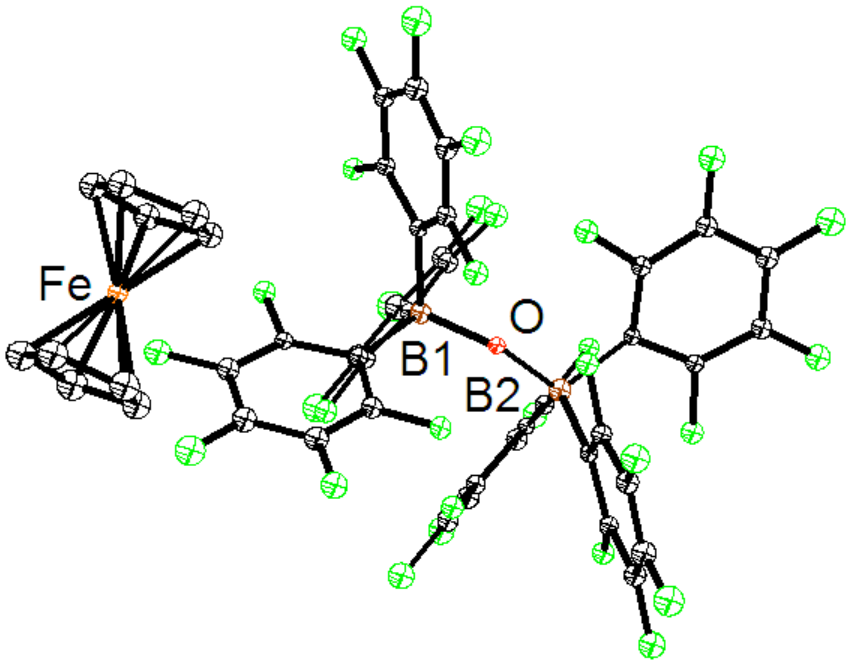

Figure 36. Preliminary crystal structure of $[\{(F_5C_6)_3B\}_2OH^-][Cp_2Fe^+]\bullet 2CH_2Cl_2$. Hydrogen atoms and solvent molecules not shown for clarity. Carbon and fluorine atoms shown in black and green, respectively.

References

1. Dembech, P.; Ricci, A.; Seconi, G.; Taddei, M. *Org. Synth.* **1997**, *74*, 84.
2. Brookhart, M.; Grant, B.; Volpe, A.F. *Organometallics* **1992**, *11*, 3920-3922.
3. APEX2, Version 2 User Manual, M86-E01078, Bruker Analytical X-ray Systems, Madison, WI, June 2006.
4. Sheldrick, G.M. "SADABS (version 2008/1): Program for Absorption Correction for Data from Area Detector Frames", University of Göttingen, 2008.
5. Sheldrick, G.M. (2008). Acta Cryst. A64, 112-122.
6. Brandenburg, K. (1999). DIAMOND. Crystal Impact GbR, Bonn, Germany.